Malaysian Journal of Chemistry, 2026, Vol. 28(3), 61-69
(Special Issue: *2nd International Conference on Advanced Materials & Sustainable Energy Technologies, AMSET 2025*)

Volumetric Interaction Mechanisms in 2-Ethylhexylamine–DMSO Mixtures for CO_2 Capture: Experimental Excess Molar Volume Analysis and COSMO-RS Modelling

Mohd Azlan Kassim[1]*, Abdul Azim Abdul Manam[2] and Rozita Yusoff[2]
[1]Research Centre of Carbon Dioxide Capture and Utilisation (CCDCU), Faculty of Engineering and Technology, Sunway University, Bandar Sunway, 47500 Petaling Jaya, Malaysia
[2]Chemical Engineering Department, Faculty of Engineering, University of Malaya, 50603 Kuala Lumpur, Malaysia
*Corresponding author (e-mail: azlanka@sunway.edu.my)

Understanding the volumetric properties of a solvent system is crucial for developing and optimising CO_2 absorption processes for efficient CO_2 capture. Hence this study explores volumetric properties for binary mixtures of 2-ethylhexylamine (EHA) and dimethyl sulfoxide (DMSO) for CO_2 absorption. The experimental density data, ρ, collected over the whole mixture composition at temperatures 298.15 K to 353.15 K, were used to calculate excess molar volumes (V_m^E). Subsequently correlated using the Redlich-Kister polynomial equation. A negative V_m^E values were observed at lower EHA composition, while, a positive V_m^E values were observed at high EHA composition in the binary mixtures system indicating compression and expansion of volume due to interaction between EHA and DMSO in the binary mixtures system throughout the composition range. Subsequently, COSMO-RS modelling was applied to deduce the molecular interactions.

Keywords: Redlich-Kister, excess molar volume, EHA, DMSO, COSMO-RS model

Received: February 2026; Accepted: April 2026

The increasing atmospheric carbon dioxide (CO_2) concentration, predominantly driven by burning of non-renewable fuel source for transportation and energy generation purposes, remains the most significant cause to global climate change. Hence, Carbon Capture and Storage (CCS) technologies have been prioritized globally to moderate the adverse environmental affects of greenhouse gas emissions [1, 2]. Among various capture methodologies, post-combustion capture using liquid chemical absorption is widely regarded as the most mature and commercially viable approach. While traditional alkanolamines, such as monoethanolamine (MEA), have long served as the industry standard, they are often hindered by high energy requirements for regeneration, susceptibility to oxidative degradation, and equipment corrosion [1-3]. Consequently, recent research has shifted toward the development of "hybrid" solvent systems that incorporate the high reactivity of amines with the physical advantages of organic solvents [1, 2, 4, 5].

One such promising candidate is 2-ethylhexyl-amine (EHA), a primary amine characterized by its hydrophobic nature and potential for high CO_2 loading. To optimize the performance of EHA in industrial applications, it is frequently blended with physical co-solvents like Dimethyl Sulfoxide (DMSO) [4, 5]. DMSO is a versatile, polar aprotic solvent known for its high thermal stability, low toxicity, and ability to enhance gas solubility, making it an excellent medium for modulating the viscous and thermodynamic properties of amine-based catchments [6, 7]. Experimental studies have demonstrated that EHA-DMSO formulations achieve high cyclic capacity, excellent desorption efficiency, and approximately 50% lower estimated desorption-energy consumption compared to 30 wt% MEA, with no phase separation after absorption [4, 5].

Designing and scaling CO_2 absorption columns effectively rely on a precise understanding of the solvent mixtures' volumetric and thermophysical properties. Properties such as density (ρ) and excess molar volume (V_m^E) are not merely engineering parameters; they serve as a window into the molecular-level interactions occurring within the liquid phase [7, 8]. The deviation of a real mixture from ideal behaviour, as quantified by V_m^E, provides critical insights into the underlying forces—such as hydrogen bonding, dipole-dipole interactions, and steric hindrance—that dictate the solvent's macro-scale performance [7-9].

This study aims to provide comprehensive experimental data on densities and excess molar volumes for EHA (1) + DMSO (2) systems at different temperatures, and to analyze these data in relation to molecular interactions within the mixtures. The COSMO-RS model is employed to predict the σ-profile for the mixture compositions. Thermophysical

†Paper presented at the 2nd International Conference on Advanced Materials & Sustainable Energy Technologies 2025

data, such as density, are essential in the chemical industry for process design and optimisation, including the determination of mass transfer, fluid flow, heat transfer, and energy consumption [10-12]. Additionally, thermophysical property data are valuable for understanding intermolecular interactions within mixtures.

EXPERIMENTAL

Material

Table 1 details and Figure 1 illustrated the chemicals used in this work. The chemicals are used as received.

Method

Apparatus and Procedure

The binary mixtures' density were determined using the calibrated densitometer DMA 45000 M (Anton Paar, Germany). Measurements were conducted at atmospheric pressure at temperature ranging from 298.15 K to 353.15 K.

Computational Details

EHA and DMSO was evaluated using the COSMO-RS approach. Geometry optimization was performed for each of species involved using the Density Functional Theory (DFT) BP86 level and triple-zeta valence potential (TZVP) basis set. Single point energy calculation BP86 def2-TZVPD FINE basis set was conducted utilizing the geometrical optimized structure in generating the *.cosmo* file. The geometry optimization and single point calculation were performed using TMoleX quantum chemistry program package. While the COSMO-RS calculations were performed using the COSMOthermX software package.

Table 1. The sample provenance table for the compounds system[a].

Chemical	EHA	DMSO
Molecular formula	$C_8H_{19}N$	CH_6OS
IUPAC name	2-ethylhexan-1-amine	methylsulfinylmethane
CASRN	104-75-6	67-68-5
Source	Merck	Merck
Purity grade	AR	AR
Mass fraction purity	0.99	0.99
Purification Method	None	None
Analysis Method	GC	GC
Water (wt%)	0.295	0.461

[a]All materials are used without further purifications

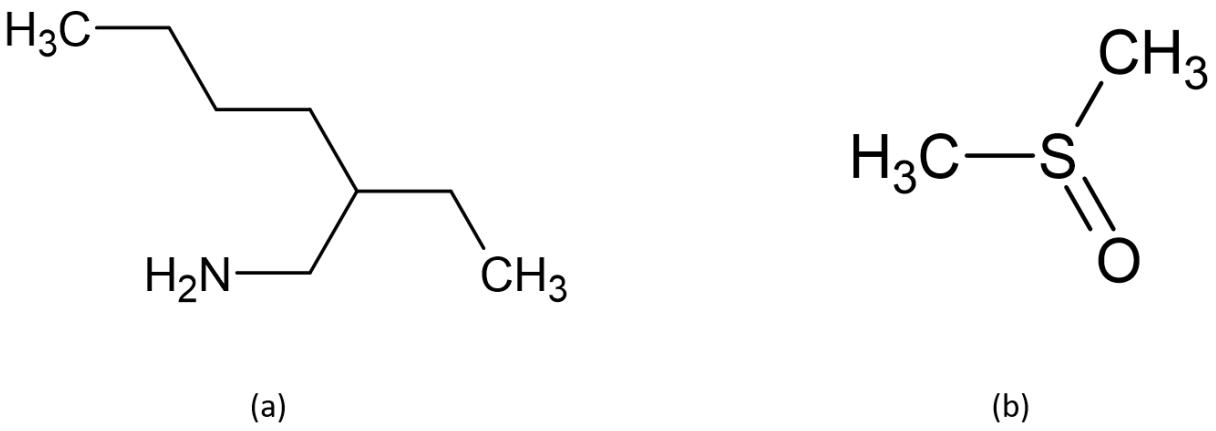

Figure 1. Chemical structures of; (a) EHA and (b) DMSO.

Table 2. Validation of Measured Densities (ρ) EHA and DMSO against literature data.

ρ, g cm^{-3}	EHA		DMSO	
T/K	**Exp.**	**Lit.[1]**	**Exp.**	**Lit.[2]**
298.15	0.78436	0.78501	1.09537	1.0961
303.15	0.78032	0.78188	1.09042	
313.15	0.77.221	0.77294	1.08041	
323.15	0.76406	0.76535	1.07032	1.07300
333.15	0.75591	0.75714	1.06026	1.06230
343.15	0.74770	0.74928	1.05022	1.05130
353.15	0.73950	0.74006	1.04010	

1 = data from [13]
2 = data from [14]

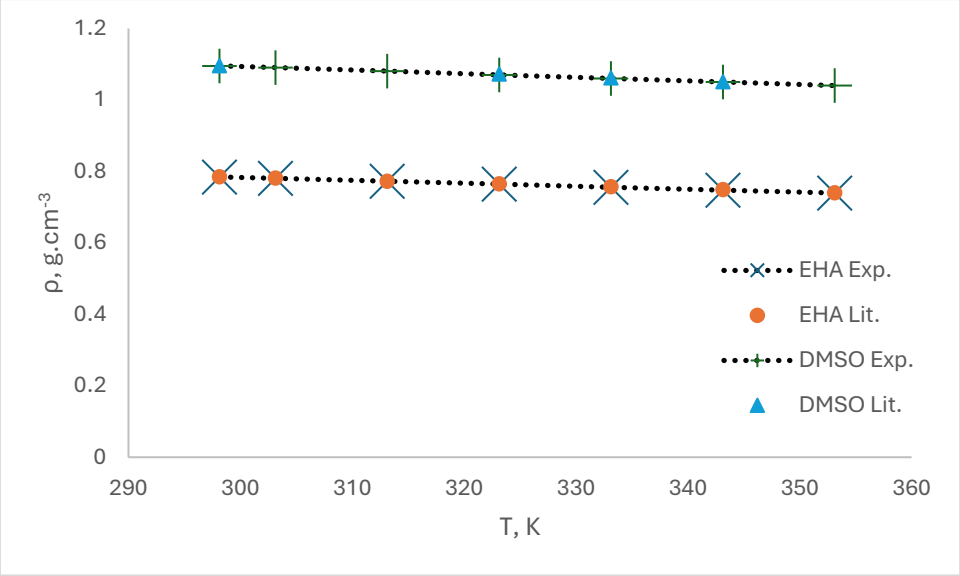

Figure 2. Comparison of experimental and literature density (ρ) values for EHA and DMSO as a function of temperature.

RESULTS AND DISCUSSION

Pure Compounds and Their Binary Mixtures

The reliability of the experimental apparatus and methodology was confirmed by measuring the densities of pure EHA and DMSO at multiple temperatures, then comparing these findings with published literature data (Table 2); the relative deviations, calculated using Equation (1), are plotted in Figure 2.

$$Relative\ Deviation = \frac{Y_{exp} - Y_{lit}}{Y_{exp}},\ Y = \rho \qquad (1)$$

where ρ is the density. The subscript "exp" and "lit" denote experimental data of this work and literature values, respectively.

The experimental densities for the EHA (1) + DMSO (2) binary system, presented in Table 3 and Figure 3, demonstrate that density is inversely proportional to both EHA mole fraction and temperature. Specifically, the density exhibits a quasi-linear decline with rising temperature across the entire composition range.

Table 3. Density (ρ) and excess molar volume (V_m^E) data for EHA + DMSO mixtures at atmospheric pressure and multiple temperatures.

EHA (1) + DMSO (2)			
x_1	x_2	ρ (g cm^{-3})	V_m^E (cm^3 mol^{-1})
T = 298.15 K			
0.0000	1.0000	1.0954	0
0.1001	0.8999	1.041256	-0.52924
0.2000	0.8000	0.992436	-0.594
0.3000	0.7000	0.948962	-0.27573
0.4000	0.6000	0.910812	0.314261
0.4999	0.5001	0.878003	1.033773
0.6000	0.4000	0.850515	1.712673
0.6999	0.3001	0.828365	2.156811
0.8000	0.2000	0.811549	2.158211
0.8998	0.1002	0.800061	1.506324
1.0000	0.0000	0.7939	0
T = 303.15 K			
0.0000	1.0000	1.0904	0
0.1001	0.8999	1.036614	-0.55426
0.2000	0.8000	0.988088	-0.64121
0.3000	0.7000	0.944844	-0.34138
0.4000	0.6000	0.90686	0.235047
0.4999	0.5001	0.874153	0.94709
0.6000	0.4000	0.846703	1.625838
0.6999	0.3001	0.824527	2.078196
0.8000	0.2000	0.807621	2.096861
0.8998	0.1002	0.79598	1.471383
1.0000	0.0000	0.7896	0
T = 313.15 K			
0.0000	1.0000	1.08041	0
0.1001	0.8999	1.026939	-0.56556
0.2000	0.8000	0.978698	-0.65646
0.3000	0.7000	0.935709	-0.3541
0.4000	0.6000	0.89795	0.22988
0.4999	0.5001	0.865438	0.9525
0.6000	0.4000	0.838153	1.642276
0.6999	0.3001	0.816112	2.103036
0.8000	0.2000	0.799311	2.124072
0.8998	0.1002	0.787745	1.491428
1.0000	0.0000	0.78141	0
T = 323.15 K			
0.0000	1.0000	1.07032	0
0.1001	0.8999	1.017164	-0.57749
0.2000	0.8000	0.969208	-0.67261
0.3000	0.7000	0.926474	-0.36771
0.4000	0.6000	0.88894	0.224108
0.4999	0.5001	0.856623	0.957765
0.6000	0.4000	0.829503	1.65909
0.6999	0.3001	0.807597	2.128691
0.8000	0.2000	0.790901	2.152294
0.8998	0.1002	0.779409	1.512267
1.0000	0.0000	0.77312	0
T = 333.15 K			
0.0000	1.0000	1.06026	0
0.1001	0.8999	1.00742	-0.587625161
0.2000	0.8000	0.959752	-0.685211972

0.3000	0.7000	0.917278	-0.376147581
0.4000	0.6000	0.879976	0.224839421
0.4999	0.5001	0.847863	0.970423766
0.6000	0.4000	0.820919	1.683582657
0.6999	0.3001	0.799161	2.161541378
0.8000	0.2000	0.782585	2.18632089
0.8998	0.1002	0.771185	1.536522701
1.0000	0.0000	0.76496	0
T = 343.15 K			
0.0000	1.0000	1.05022	0
0.1001	0.8999	0.997686	-0.59945
0.2000	0.8000	0.950296	-0.70072
0.3000	0.7000	0.908072	-0.38822
0.4000	0.6000	0.870992	0.221705
0.4999	0.5001	0.839073	0.979432
0.6000	0.4000	0.812295	1.705009
0.6999	0.3001	0.790675	2.192158
0.8000	0.2000	0.774209	2.219034
0.8998	0.1002	0.762891	1.560279
1.0000	0.0000	0.75672	0
T = 353.15 K			
0.0000	1.0000	1.0401	0
0.1001	0.8999	0.98789	-0.61343
0.2000	0.8000	0.940792	-0.72032
0.3000	0.7000	0.898828	-0.40598
0.4000	0.6000	0.861976	0.211689
0.4999	0.5001	0.830253	0.980908
0.6000	0.4000	0.803639	1.718895
0.6999	0.3001	0.782151	2.215955
0.8000	0.2000	0.765785	2.246433
0.8998	0.1002	0.754535	1.581013
1.0000	0.0000	0.7484	0

[a] Standard uncertainty u is u(x) = 0.0005, u(T) = 0.05 K, $u(\rho)$ = 0.001 g cm^{-3}, u(P) = 0.5 kPa and combined expanded uncertainties (confidence level, 95%) U(V^E) = 0.0001 cm^3 mol^{-1}.

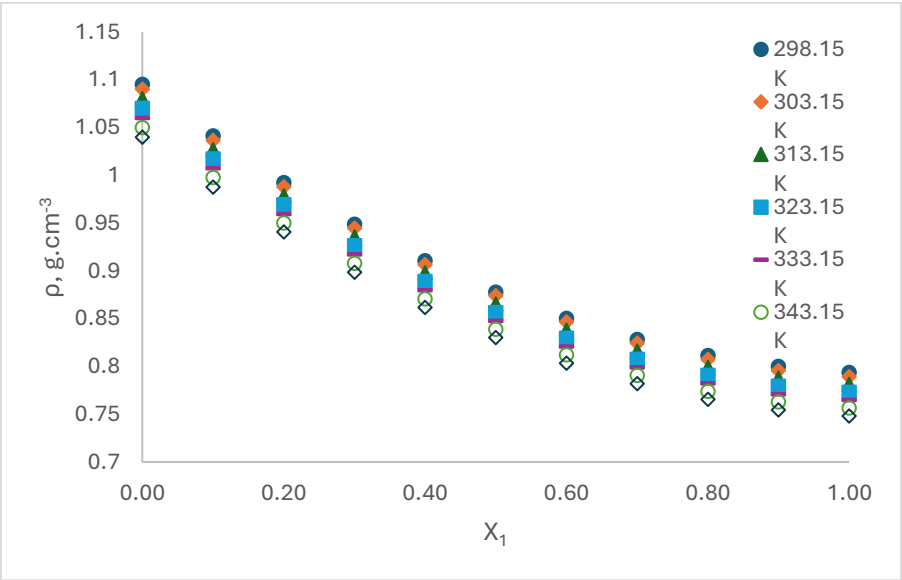

Figure 3. Density profiles of EHA (1) + DMSO (2) mixtures at various temperatures.

Excess Molar Volume

The excess molar volume (V_m^E) was determined from experimental mixture densities (ρ) and pure component densities (ρ_i) by incorporating the respective mole fractions (x_i) and molar masses (M_i) into Equation 2 [15].

$$V_m^E = x_1 M_1 \left(\frac{1}{\rho} - \frac{1}{\rho_1}\right) + x_2 M_2 \left(\frac{1}{\rho} - \frac{1}{\rho_2}\right) \quad (2)$$

Table 3 summarized excess molar volume values and represented by Figure 4 using a Redlich-Kister Equation 3 [16] where Y^E represent the excess properties:

$$Y^E = x_1 x_2 \sum_{i=0}^{n} A_i (2x_1 - 1)^i \quad (3)$$

where A_i refers to the adjustable parameter and n is the number of coefficients in the equation. Table 4 tabulated the adjustable parameters, A_i.

Figure 4 shows the thermodynamic behaviour of EHA (1) + DMSO (2) binary mixture across a temperature range. The experimental results reveal a distinct S-shaped dependency on the mole fraction of EHA (x_1), indicating significant non-ideal behaviour and a complex interplay of molecular forces. At lower EHA concentrations ($x_1 < 0.4$), the mixture exhibits negative V^E values, showing a net contraction in the molar volume. This contraction is primarily attributed to enhanced molecular packing efficiency facilitated by strong intermolecular attractions between the components. Specifically, the highly polar and amphiprotic nature of DMSO allows for favourable dipole-dipole interactions and van der Waals forces with the aliphatic backbone and ester groups of the EHA molecules. These attractive forces effectively pull the unlike molecules closer together than they would be in an ideal state, thereby reducing the total volume of the solution. As the composition of EHA increases beyond the equimolar point, the system moves toward positive V_m^E values, representing a net expansion of the mixture. This phenomenon is driven by two primary mechanisms: the disruption of self-associated networks and steric hindrance. The introduction of DMSO molecules into an EHA-rich environment facilitates the breakage of intramolecular hydrogen bonding within EHA clusters. Furthermore, the presence of the bulky, flexible 2-ethylhexyl alkyl chains hinders tight molecular alignment, resulting in increased steric repulsion and the creation of larger interstitial voids. Consequently, the expansion caused by these repulsive forces and the loss of cohesive interaction outweighs any remaining contraction effects, leading to the observed positive deviation. Overall, the V_m^E profile highlights a concentration-dependent transition from packing-dominated contraction to expansion driven by steric bulk and structural disruption.

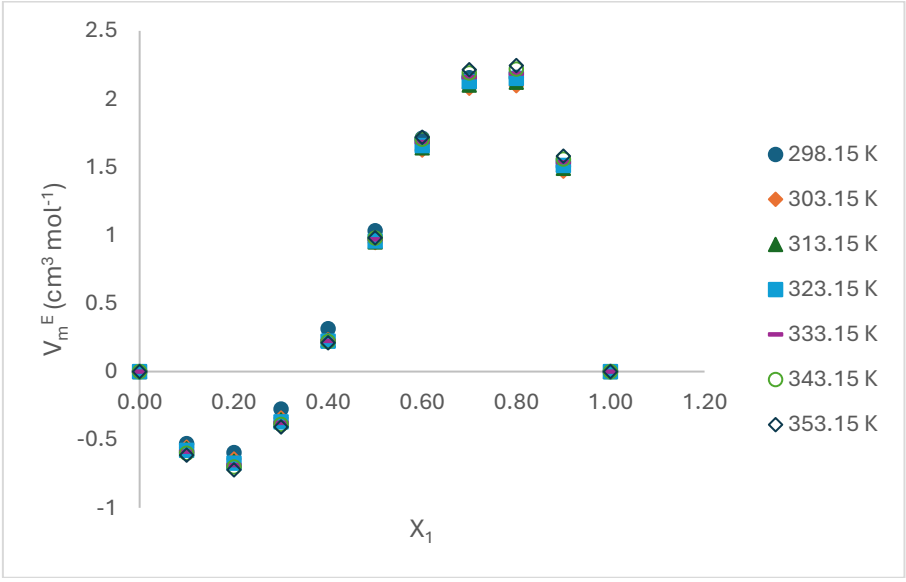

Figure 4. Excess molar volume profiles of EHA (1) + DMSO (2) mixtures at various temperatures as function of EHA mol fraction.

Table 4. Redlich-Kister fitting coefficients A_i of the V_m^E of EHA (1) + DMSO (2) binary mixtures.

T / K	A_0	A_1	A_2	A_3	A_4	R^2	σ^a
303.15	2.0569	-0.7691	-0.0835	3.1342	0.2938	0.9995	0.0056
313.15	3.2035	-0.4493	1.0760	6.6596	1.4246	0.9993	0.0113
323.15	2.4946	-0.5052	0.0721	2.3582	-1.1761	0.9975	0.0153
333.15	2.6907	-0.8461	0.2010	2.7630	-1.6736	0.9979	0.0153

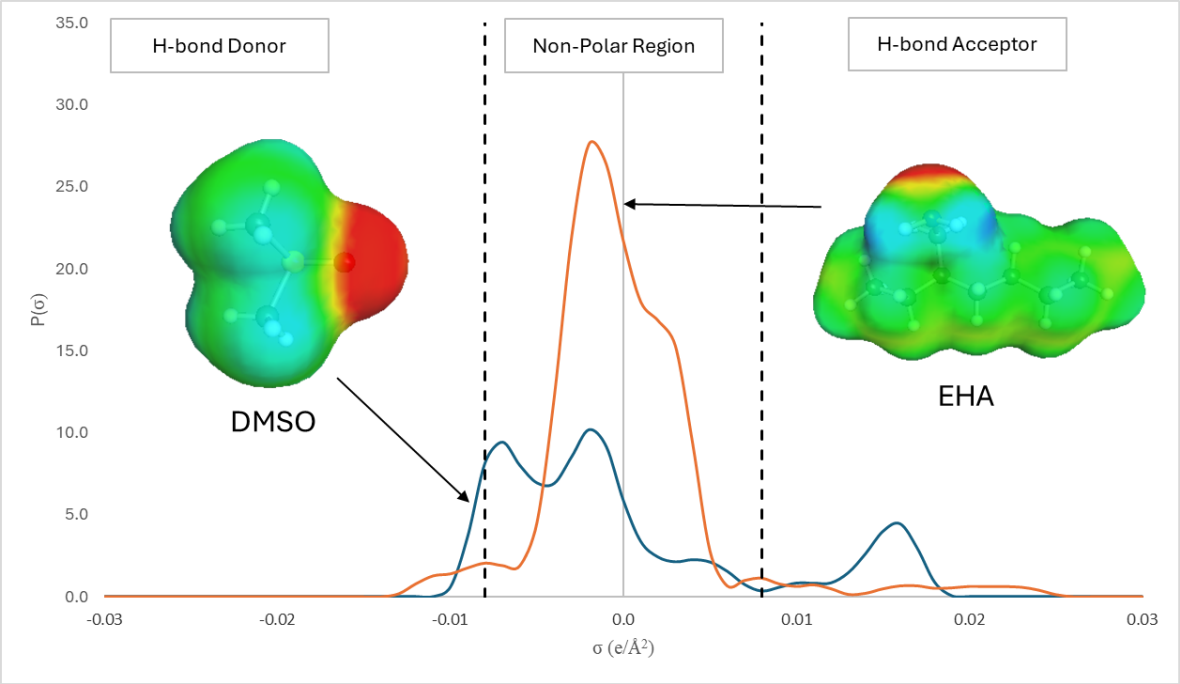

Figure 5. Surface charge density distributions (σ-profile) of EHA and DMSO calculated via COSMO-RS.

COSMO-RS Modelling

To further elucidate molecular interactions within EHA (1) and DMSO (2) binary mixtures, the COSMO-RS model was employed to calculate 3D polarized charge distributions (σ) on each component's molecular surface. These screening charges are visualized via σ-profile histograms, which serve as qualitative descriptors to predict potential liquid-phase interactions by categorizing the molecular surface into three distinct functional zones: the hydrogen bond donor region ($\sigma < -0.0082$ e/Å^2), the hydrogen bond acceptor region ($\sigma > 0.0082$ e/Å^2), and the non-polar region ($-0.0082 < \sigma < 0.0082$ e/Å^2). As illustrated in Figure 5, these profiles provide a theoretical basis for understanding the chemical affinities between EHA and DMSO.

σ-profile for EHA is dominated by a main peak at $\sigma \approx 0$ e/Å^2 in the non-polar region of the histogram illustrates the long aliphatic alkyl chain backbone of EHA structure (green), while small, broader peaks in the H-bond acceptor region indicates the polar lone pair on the nitrogen atom (red). while the peak in the hydrogen bond acceptor region indicates the polar sulfonyl group (red). EHA shows a distinct peak in H-bond donor region which corresponds to the hydrogens attached to the nitrogen in the primary amine group

The σ-profile of DMSO shows a much lower peak in the non-polar region, due to it is a small molecule with only two methyl groups, making it significantly less hydrophobic than EHA In the hydrogen-bond donor region, DMSO exhibit a significant, sharp peak around $\sigma \approx 0.016$ e/Å^2 which represents the highly electronegative oxygen atom in the S=O bond, which is a very strong H-bond acceptor. In the other hand, DMSO has negligible activity in the H-bond donor region due to lacks of acidic hydrogens.

The molecular interactions within the EHA (1) + DMSO (2) binary system are characterized by a competition between polar attractions and steric effects, resulting in a distinct transition from negative to positive V^E. At low EHA mole fractions ($x_1 < 0.5$), the system exhibits volume contraction ($V^E < 0$), which is primarily attributed to strong intermolecular interactions between the highly polar, amphiprotic DMSO and the amine groups of EHA. As evidenced by COSMO-RS σ-profiles, the alignment of DMSO's donor regions with EHA's acceptor sites facilitates a high degree of molecular packing efficiency and van der Waals stabilization. At a higher EHA concentration ($x1 > 0.5$), the mixture undergoes volume expansion ($V^E > 0$). This shift is driven by the dominance of the long, non-polar alkyl chains of EHA, which introduce significant steric hindrance and prevent tight molecular packing. The increasing concentration of EHA disrupts the cohesive DMSO–DMSO dipole-dipole networks, replacing them with weaker EHA–EHA and EHA–DMSO interactions. This disruption, coupled with the inability of the bulky alkyl chains to fill the resulting molecular voids, leads to an increase in the total free volume of the mixture.

CONCLUSION

In this work, we have measured the density measurement and calculate the excess molar volume for EHA (1) + DMSO (2) binary mixtures over whole range of composition at different temperature, 298.15 K to 353.15 K. The experimental data reveals that the mixture exhibits a characteristic S-shaped curve for excess molar volume, indicating a significant deviation from ideal behaviour. Specifically, at lower EHA (1) concentrations, a negative excess molar volume is observed due to volume contraction, signalling an increased interaction between the EHA and DMSO components. Conversely, at higher EHA (1) concentrations, the system demonstrates a positive excess molar volume resulting from volume expansion, which indicates a transition toward weaker molecular interactions. This complex behaviour of the binary solutions is further justified through COSMO-RS analysis, utilizing the σ-profile of each component to provide a molecular-level understanding of the phase behaviour and intermolecular forces at play.

ACKNOWLEDGEMENT

The author would like to extend their gratitude to Sunway University for awarding this project under the Internal Grant Scheme (IGS) 2023 (GRTIN-IGS(02)-CCDCU-07-2023).

REFERENCES

1. Zheng, R. F., Barpaga, D., Mathias, P. M., Malhotra, D., Koech, P. K., Jiang, Y., Bhakta, M., Lail, M., Rayer, A. V., Whyatt, G. A., Freeman, C. J., Zwoster, A. J., Weitz, K. K. and Heldebrant, D. J. (2020) A single-component water-lean post-combustion CO2 capture solvent with exceptionally low operational heat and total costs of capture – comprehensive experimental and theoretical evaluation. *Energy & Environmental Science,* **13(11)**, 4106–4113.

2. Zhang, S., Shen, Y., Shao, P., Chen, J. and Wang, L. (2018) Kinetics, Thermodynamics, and Mechanism of a Novel Biphasic Solvent for CO2 Capture from Flue Gas. *Environmental Science & Technology*, **52(6)**, 3660–3668.

3. Mohd Rasdi, F. L., Jeyaseelan, R., Taha, M. F. and Mohd Razip, M. A. A. (202) Optimization of CO2 Capture Using a New Aqueous Hybrid Solvent (MDEA-[TBPA][TFA]) with a Low Heat Capacity: Integration of COSMO-RS and RSM Approaches. *Processes*, **12(12)**, 2626.

4. Meng, F., Fu, K., Wang, X., Wang, Y., Wang, L. and Fu, D. (2024) Study on absorption and regeneration performance of EHA-DMSO non-aqueous absorbent for CO2 capture from flue gas. *Energy*, **286**, 129631.

5. Kassim, M. A., Ho, Z., Hussin, F. and Arou, M. K. (2024) Exploring Non-aqueous Solutions for CO2 Capture at Elevated Pressure: An Initial Study for EHA/MOR in DMSO Mixtures. *E3S Web of Conf.*, **488**, 03024.

6. Andreatta, A. E., Florusse, L. J., Bottini, S. B. and Peters, C. J. (2007) Phase equilibria of dimethyl sulfoxide (DMSO)+carbon dioxide, and DMSO+carbon dioxide+water mixtures. *The Journal of Supercritical Fluids*, **42(1)**, 60–68.

7. Wang, J., Long, Q., Wang, S. and Shen, S. (2024) Measurement and Modeling of Thermophysical Properties of the Ternary System 2-(Butylamino) ethanol + Dimethyl Sulfoxide + Water and Its Binary Subsystems. *Journal of Chemical & Engineering Data*, **69(9)**, 3017–3028.

8. Zhao, B., Liu, L.,Yang, X., Liu, C., Sha, F. and Zhang, J. (2017) Liquid density, viscosity and spectroscopic studies of binary mixture of tetraethylene glycol + 1,2-ethanediamine for CO2 capture. *Physics and Chemistry of Liquids*, **55(6)**, 715–730.

9. Das, D., Barhoumi, Z. and Ouerfelli, N. (2012) The relative reduced Redlich–Kister equations for correlating excess properties of N,N-dimethylacetamide + 2-methoxyethanol binary mixtures at temperatures from 298.15 K to 318.15 K. *Physics and Chemistry of Liquids*, **50(3)**, 346–366.

10. Tariq, M., Carvalho, P. J., Coutinho, J. A. P., Marrucho, I. M., Canogia Lopes, J. N. and Rebelo, L. P. N. (2011) Viscosity of (C2–C14)

1-alkyl-3-methylimidazolium bis(trifluoromethyl sulfonyl)amide ionic liquids in an extended temperature range. *Fluid Phase Equilibria*, **301(1)**, 22–32.

11. Abd Ghani, N., Sairi, N. A., Aroua, M. K., Alias, Y. and Yusoff, R. (2014) Density, Surface Tension, and Viscosity of Ionic Liquids (1-Ethyl-3-methylimidazolium diethylphosphate and 1,3-Dimethylimidazolium dimethylphosphate) Aqueous Ternary Mixtures with MDEA. *Journal of Chemical & Engineering Data*, **59(6)**, 1737–1746.

12. Wan Normazlan, W. M. D., Sairi, N. A., Alias, Y., Udaiyappan, A. F., Jouyban, A. and Khoubnasabjafari, M. (2014) Composition and Temperature Dependence of Density, Surface Tension, and Viscosity of EMIM DEP/MMIM DMP + Water + 1-Propanol/2-Propanol Ternary Mixtures and Their Mathematical Representation Using the Jouyban–Acree Model. *Journal of Chemical & Engineering Data*, **59(8)**, 2337–2348.

13. Harris, K. R., Kanakubo, M. and Woolf, L. A. (2007) Temperature and pressure dependence of the viscosity of the ionic liquids 1-hexyl-3-methylimidazolium hexafluorophosphate and 1-butyl-3-methylimidazolium bis(trifluoromethyl sulfonyl)imide. *Journal of Chemical & Engineering Data*, **52(3)**, 1080–1085.

14. Amundsen, T. G., Øi, L. E. and Eimer, D. A. (2009) Density and viscosity of monoethanolamine + water + carbon dioxide from (25 to 80) °C. *Journal of Chemical & Engineering Data*, **54(11)**, 3096–3100.

15. Zarei, H., Golroudbari, S. A. and Behroozi, M. (2013) Experimental studies on volumetric and viscometric properties of binary and ternary mixtures of N,N-dimethylacetamide, N-methylform amide and propane-1,2-diol at different temperatures. *Journal of Molecular Liquids*, **187**, 260–265.

16. Vranes, M., Zec, N., Tot, A., S., Dožić, S. and Gadžurić, S. (2014) Density, electrical conductivity, viscosity and excess properties of 1-butyl-3-methylimidazolium bis(trifluoromethylsulfonyl) imide plus propylene carbonate binary mixtures. *Journal of Chemical Thermodynamics*, **68**, 98–108.

17. Gonzalez-Miquel, M., Massel, M., DeSilva, A., Palomar, J., Rodriguez, F. and Brennecke, J. F. (2014) Excess enthalpy of monoethanolamine + ionic liquid mixtures: How good are COSMO-RS predictions? *The Journal of Physical Chemistry B*, **118(39)**, 11512–11522.